https://www.scientificarchives.com/journal/archives-of-proteomics-and-bioinformatics

Archives of Proteomics and Bioinformatics Research Article

Antisense Inhibition of *accA* in *E. coli* Suppressed *luxS* Expression and Increased Antibiotic Susceptibility

Tatiana Hillman*

Biotechnology, TheLab Inc., Los Angeles, California, United States

*Correspondence should be addressed to Tatiana Hillman; thillman@thel4binc.org

Received date: April 20, 2021, **Accepted date:** June 04, 2021

Abstract

Bacterial multidrug resistance (MDR) is a significant issue in the medical community. Gram-negative bacteria (GNB) exhibit higher rates of MDR, partly due to the impermeability of the GNB double membrane cell envelope, which limits the internal accumulation of antibiotic agents. In *Escherichia coli*, a GNB, the genes *accA* and *accD*, produce the AccA and AccD subunits of the acetyl-CoA carboxylase transferase enzyme that is essential for catalyzing fatty acid synthesis (FAS). FAS produces phospholipids that comprise the double membrane required for forming viable and antibiotic resistant GNB. Therefore, FAS affects the composition of GNB cell membranes and can alter antibiotic susceptibility. However, the association between fatty acid metabolism, virulence, and antibiotic uptake requires further elucidation. For this reason, the current study investigated the link between fatty acid metabolism, virulence, and antibiotic susceptibility by disrupting FAS in *E. coli* via antisense RNA (asRNA) inhibition of *accA*. Suppression of FAS through asRNA inhibition of *accA*, downregulated *luxS*, which is a vital virulence factor for mediating pathogenic bacterial quorum sense (QS) signaling and decreased antibiotic resistance in *E. coli*. The results of this study confirm that *accA* is a potent target for developing novel antimicrobial gene therapies.

Keywords: Antibiotic resistance; Antibiotics; Carboxylase enzymes; Autoinducers; Quorum sense; Antisense RNA; Fatty acid synthesis

Introduction

Multidrug resistant (MDR) bacteria, which are resistant to more than one antibiotic, present an enormous challenge for medical communities and organizations worldwide. For example, *Acinetobacter baumannii* is a highly contagious MDR gram-negative bacterium (GNB) that inhabits hospitals and causes 64% of urinary tract infections associated with the use of catheters [1]. Alexopoulou et al. found that there were more healthcare-associated infections caused by GNB than Gram-positive Cocci (GPC) bacteria, in which 81% were GNB infections and 42% were caused by GPC bacteria [2]. Many cases of MDR are caused by gram-negative bacteria, which have a double-membrane cell envelope that provides partial protection from diffusible hydrophobic and hydrophilic compounds [3,4]. The gram-negative bacterial cell envelope consists of an inner membrane (IM) with a phospholipid bilayer, periplasmic space, and an outer membrane, which provide a lipopolysaccharide (LPS) region [4]. LPS blocks the influx of hydrophobic and hydrophilic molecules, while the IM constrains the internal transport of hydrophilic molecules, thereby limiting the accrual of antibiotics and enzyme inhibitors within the bacterial cell. This presents obstacles for discovering additional antibacterial drugs to inhibit the growth of Gram-negative pathogens, because many potent enzyme blockers cannot efficiently accumulate inside of the cell [5].

The inner membrane (IM) of Gram-negative cell envelopes consists of a phospholipid (PL) bilayer composed through type II fatty acid synthesis (FASII) [5]. FASII proteins include the acetyl-CoA carboxylase (ACCase) complex, which is an essential enzyme for the first rate-limiting step in fatty acid synthesis. ACCase consists of three subunits: a dimerized biotin-dependent carboxylase (BC), a biotin carboxyl carrier protein (BCCP), and an α2β2heterotetrameric carboxyltransferase (CT) [6-10]. The genes encoding the ACCase complex are *accA* and *accD*, which encode the α and β subunits of CT; *accB*

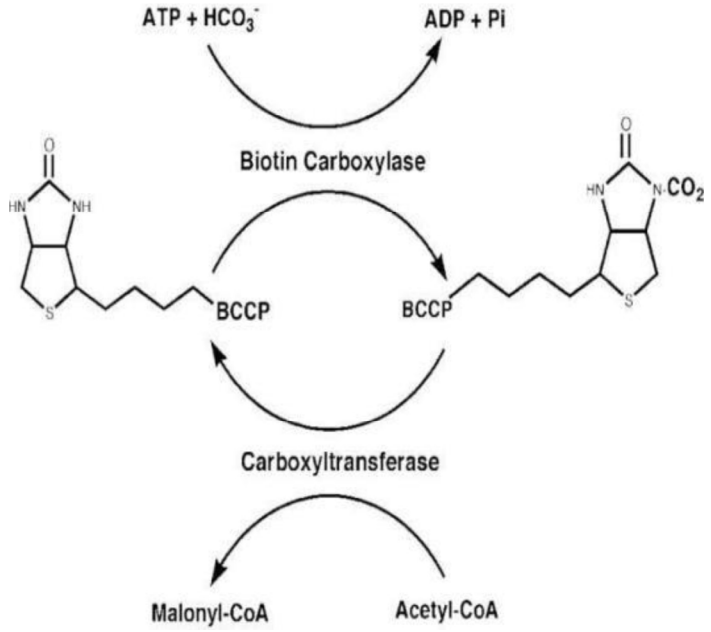

Figure 1: Formation of Malonyl-CoA (produced from reference [13] and originally published in the Journal of Biological Chemistry Creative Commons CC-BY-NC-ND). The alpha and beta subunits of the AccABCD complex transfer a carboxyl group from pyruvate to acetyl-CoA, forming malonyl-CoA. The carboxylate moiety is carried by biotin covalently bound to BCCP through the action of a biotin carboxylase (BC)with ATP and carbon dioxide from bicarbonate as cofactors. In the second step of the reaction, a carboxyltransferase (CT) transfers carbon dioxide from carboxybiotin to a carboxyl group and then moves the carboxyl group to acetyl-CoA, producing malonyl-CoA.

(BCCP) and *accC* (BC), respectively. Of these, *accB* and *accC* are transcribed simultaneously via the *accBC* mini operon [11]. In the first phase of FASII, carboxylation of acetyl-CoA by BCCP and CT produces malonyl-CoA. Specifically, the AccAD subunit transfers a carboxyl delivered through BC-BCCP to CT, BC-BCCP positions a carboxyl taken from a glucose-derived pyruvate for CT, and CT orients the carboxyl to acetyl-CoA, enabling the synthesis of malonyl-CoA (Figure 1). Subsequently, malonyl-CoA is converted to malonyl-ACP and then combined with acetyl-CoA by the enzyme 3-oxoacyl-[acyl-carrier-protein] synthase 3 (FabH) in an ATP-dependent reaction to generate ketoacyl-ACP [12]. FASII is initiated when the CT enzyme catalyzes fatty acid elongation, which adds two carbons per cycle of the FAS process.

When ACCase malfunctions, fatty acid synthesis is blocked, and carbohydrate metabolism is disrupted, causing damage to bacterial cells [14]. The herbicides, haloxyfop and arylophenoxypropionate, inhibited AccD6 of the ACCase-CT enzyme and showed *in vitro* suppression of *M. tuberculosis* [15]. Gene silencing of target-specific inhibitor sites of FASII confirms that the FASII pathway is essential for the survival of bacterial cells [16]. Therefore, the bacterial FASII pathway is a confirmed and validated target for designing new antibiotics [14]. However, gene silencing methods for reversing antibiotic resistance remain in the early phases of development, with many obstacles still present, such as the on-target delivery of gene editing technologies [17]. Additionally, the metabolic fluxes, which affect bacterial virulence, requires further elucidation. The link between bacterial metabolism and virulence requires further research and discussion because Stokes et al. confirmed that we are currently in the early stages of understanding the link between bacterial metabolism and antibiotic efficacy [18-26]. An improved understanding of the interaction between bacterial metabolic potency and virulence is required [27]. Consequently, the first objective of the current study was to disrupt FASII in *Escherichia coli* by inhibiting *accA* via antisense RNA (asRNA) transcripts.

The second objective was to ascertain the possible effects of blocking FAS activity via *accA* gene inhibition on bacterial virulence by demonstrating the interdependent activity between *accA* and *luxS*. LuxS is a potent virulence factor that induces quorum sense activity between bacteria. LuxS is an autoinducer-2 (AI-2)-producing S-ribosyl homocysteine lyase protein. LuxS produces AI-2 from the precursor molecule, 4,5-dihydroxy-2,3-pentadione (DPD). AI-2 is a signaling molecule that induces quorum sensing (QS) of bacterial cell-to-cell interactions, monitors

metabolism, assists with biofilm formation, allows the transport of metabolite molecules, and transports regulatory signals [19,28]. Inactivating AI-2 signaling molecules through a variety of mechanisms is the simplest method to inhibit the QS system, to lower bacterial antibiotic resistance, and to study new ways to develop antimicrobials [29]. Therefore, the purpose of this current study is to present evidence for the immense potential of silencing *accA* gene expression as a novel antimicrobial gene therapy. The present study demonstrates the effects of FAS inhibition on the virulence of *E. coli* by quantifying the levels of *luxS* and antibiotic resistance following *accA* gene suppression.

Hypotheses

To analyze the potential synergy between AccA and LuxS, *E. coli* asRNA inhibition of accA ((+)asRNA-*accA)*-expressing transformants were exposed to glucose molecules, after which the *luxS* gene copies were quantified by quantitative real-time PCR (qPCR) (*luxS*-qPCR). Specifically, *accA* was suppressed by interfering antisense RNAs (asRNAs), and its expression was quantified using real-time qPCR (qPCR). Antisense RNAs were designed to target sequences flanking the ribosome-binding site (RBS) and the start codon for 150-base pairs (bp) of *accA* mRNA, thereby blocking ribosomal detection and thereby inhibiting translation [30]. In addition, to test for the susceptibility of antibiotics, tetracycline-, carbenicillin-, and chloramphenicol-containing disks were implanted in *E. coli* (+)asRNA-*accA* cell agar cultures and zones of inhibition were measured. Two main hypotheses were tested in this study: 1) silencing *accA* and reducing glucose availability decreases *luxS* expression, which is an essential component of the LuxS/AI-2 QS system necessary for bacterial virulence, and 2) inhibiting *accA* increases the susceptibility of antibiotics in GNB such as *E. coli*.

Materials and Methods

Bacterial cell culture and RNA extraction

Escherichia coli (TOP10) was cultured and plated on 25 mL agar plates. The bacterial cells were inoculated into Luria-Bertani broth supplemented with glucose at concentrations of 200 µM, 50 µM, and 0 µM (173 ± 72, N=21), replicated seven times (n=7) for quantification of bacterial dsDNA. Glucose was added to the *E. coli* LB liquid cultures with concentrations of 15 mM (High-glucose), 7.5 mM (Medium-glucose), 5 mM (Low-glucose), and 0 mM (control) (48 ± 38, N=12). Antisense expression vectors were assembled using pHN1257-IPTG-PT plasmids. The antisense form of *accA* was inserted into the pHN1257-IPTG-PT plasmid. The restriction enzymes XhoI (upstream) and NcoI (downstream) were used to digest pHN1257 and the *accA* antisense gene insert for ligation (New England Biolabs, catalog no. R0146S and R0193S).

Cells transfected with recombinant pHN1257 plasmids for the asRNA of *accA* production were plated with the antibiotic kanamycin and incubated at 37°C for 24 h. Cells grown on agar plates were inoculated into 4 mL of LB liquid medium and evaluated for asRNA expression, classified as either (+) or (-)PTasRNA-*accA*. Total RNA was extracted for determining the RNA concentration of each bacterial sample. The total RNA was used to synthesize cDNA for real time qPCR analysis of *accA from E. coli* cells with 15 mM, 7.5 mM, 5 mM, and 0 mM. The cDNA for *luxS* was synthesized for qPCR analysis, using primers specific for the *luxS* gene. The RNA was extracted, and the *luxS*-cDNA was synthesized from (-)-asRNA-*accA* and (+)-asRNA-*accA* expressing *E. coli* cells with 25 µM, 5 µM, and 0 µM of glucose. Approximately, 25 total RNA extractions (N= 25, M=335.4, SD=329.2) were completed using the Omega E.Z.N.A RNA bacterial extraction kit, according to the manufacturer's instructions.

cDNA preparation

The OneScript Reverse Transcriptase cDNA Synthesis kit by Applied Biological Materials Inc. was used according to the manufacturer's instructions for cDNA preparation for both *accA* and *luxS* qPCR quantification. Total RNA was extracted from (-) and (+)asRNA-*accA E. coli* samples cultured with 15 mM, 7.5 mM, 5 mM, 25 µM, 5 µM, and a control of glucose. The cDNA/primer/RNA mix consisted of 1 µg total RNA (2 µL), 1 µL oligo(dt), 1 µL of dNTP mix (10mM), 4 µL of 5x buffer, 1 µL of RTase enzyme, 0.5 µL of RNAse inhibitor, and 10.5 µL of nuclease-free water added unto 20 µL of the total reaction volume.

PCR

PCR was performed using the Promega PCR MasterMix kit according to the manufacturer's instructions, with a reaction volume of 25 µL. Reaction-specific components consisted of upstream and downstream primers specific for the antisense *accA* gene target developed by reverse transcribing RNA into cDNA. The PCR reaction mixture consisted of 2X (5 µL) and 1X (2.5 µL) for upstream and downstream primers, less than 250 ng of cDNA template, and nuclease-free water. PCR amplification was completed in 40 cycles and PCR reactions were repeated in triplicate (n=3, N=12, 219 ± 171).

Agarose gel electrophoresis and plasmid assembly

PCR product quality in terms of primer dimers and contamination was determined by agarose gel electrophoresis. Subsequently, the PCR products and the

PTasRNA expression vector (pHN1257) were digested with the restriction enzymes XhoI (upstream) and NcoI (downstream) (New England Biolabs, catalog no. R0146S and R0193S). The *accA* PCR products were ligated into the pHN1257 plasmid by mixing 1 µL of the target DNA insert and 2 µL of the plasmids with 5 µL of the ligation mix (Takara Ligation Kit 6023). The ligation mixtures were then heat-shocked in a heat block at 90 °C for 15 min. Each ligation sample reaction was incubated for 30 min at 37 °C. A diagnostic double digest was used to confirm the insertion of the antisense of *accA* in the pHN1257 plasmid vector following ligation.

Real-time PCR

Absolute quantification by real-time qPCR was used to determine the expression levels of *accA* and *luxS*. *E. coli* pHN1257-(+)asRNA-*accA* transformants were cultured in media with glucose enhancement at concentrations of 15 mM, 7.5 mM, 5 mM, and 0 mM (N=14), and labeled as high-glucose (H-glucose), medium-glucose (M-glucose), low-glucose (L-glucose), and the control. The cDNA of *accA* synthesized from each treatment sample was diluted to 1:8 series dilutions to produce dilution curve tests for *accA*. Bacterial cells were transformed with pHN1257-(+)-asRNA-*accA* plasmids, RNA was extracted, reversed transcribed, and *luxS* expression levels were analyzed by qPCR. Approximately, 25 µM and 5 µM of glucose were added to the (+)-asRNA-*accA* bacterial samples. The (+) asRNA-*accA*-expressing cells were cultured without (-) glucose.

E. coli samples without glucose ((-)glucose) and without asRNA of *accA* ((-)asRNA-*accA*)) were the control groups. RNA was extracted from each *E. coli* bacterial sample. Approximately, 1 µg of isolated RNA was reverse transcribed into cDNA for qPCR analysis. The cDNA was diluted in a 1:10 dilution series to produce dilution curves for quantification of *luxS*. The value of *luxS* gene copies was measured using a qPCR amplification protocol (Roche LightCycler 480). The total reaction mixture volume for the qPCR analysis of each *accA* and *luxS* included: 19.2 µL of the primer pair mixture pipetted into a microcentrifuge tube carrying 240 µL of SensiMix SYBR green MasterMix, and 28.8µL of nuclease-free water. About 12µL of the SYBR green total reaction mixture was pipetted into each well containing 8 µL of the 1:8 dilution series for *accA*, 8 µL of the 1:10 dilution series for the *luxS*, into wells containing 8 µL of the unknown target DNA, and into the negative control wells. The cycle threshold values, C_t values, were recorded after qPCR analysis. The diluted standards with known concentrations were used to generate standard curves. The C_t values of each diluted standard were plotted against the known concentrations for each standard to form standard curves. The slope and y-intercept of the standard curves, including the C_t values for the unknowns, were used to calculate the gene copy number for the unknown *accA* and *luxS* gene targets.

Antibiotic resistance test

Competent T7 *E. coli* cells were transformed with the pHN1257 inducible vector expressing antisense RNA to inhibit *accA* and plated on nutrient agar medium. After transformant colony growth, 3-5 colonies were selected and cultured in LB broth for 18-24 h at 37°C in a shaking incubator. A control group that did not express asRNA for *accA* was cultured in LB broth for 24 h at 37°C. Subsequently, 100 µL of cultured broth was pipetted onto nutrient agar Petri dishes (N=64) and spread with a swab to form a bacterial lawn. Using the spread plate method formed bacterial lawns for the pHN1257-asRNA-*accA* (n=8, M ± SD, 21 ± 4, SEM=0.7, N=32) and control samples. To each plate were added disks containing 5 µL of the antibiotic for tetracycline (10 µg/mL), carbenicillin (100 µg/mL), and chloramphenicol (25 µg/mL). The bacterial cultures were then incubated for 18-24 h at 37 °C, after which the zone of inhibition for each disk (N=64) was measured in mm according to the Kirby-Bauer method and confirmed by the Clinical and Laboratory Standards Institute Disc diffusion supplemental tables for interpreting antibiotic resistance test results [31].

Statistical analysis

Descriptive analyses for the means and standard deviations were calculated using Microsoft Excel and GraphPad Prism to analyze nucleic acid production and the gene expression of *accA* after glucose addition to *E. coli* samples (N=41, M±SD, 365±220). Standard curves for the absolute quantification of *accA* (n=4, N=16, M ± SD, 48 ± 38) and *luxS* (n=3, N=12) were calculated using Microsoft Excel, where linear regression coefficients were added to each dilution series for the standard curves. The descriptive statistics and ANOVA analysis with Bonferroni and Holm results for the *p*-value of *luxS* gene copies (N=12) were computed using GraphPad Prism. The antibiotic resistance test data (N=64, M ± SD, 17.50 ± 2.00) were analyzed and subjected to unpaired *t*-tests using OriginPro 2019B to calculate the p-value ($P<0.05$, t-score=3.6, df=31, 95% CI, [6,32]). Figures illustrating the analyses were constructed using Microsoft Excel and GraphPad Prism (8th edition).

Results

Glucose and *accA* Gene expression in *E. coli*

Fatty acids could not be quantified using gas chromatography because of limited funding; therefore, FAS activity was alternatively identified. To detect FAS activity in *E. coli,* sample cultures were enhanced with

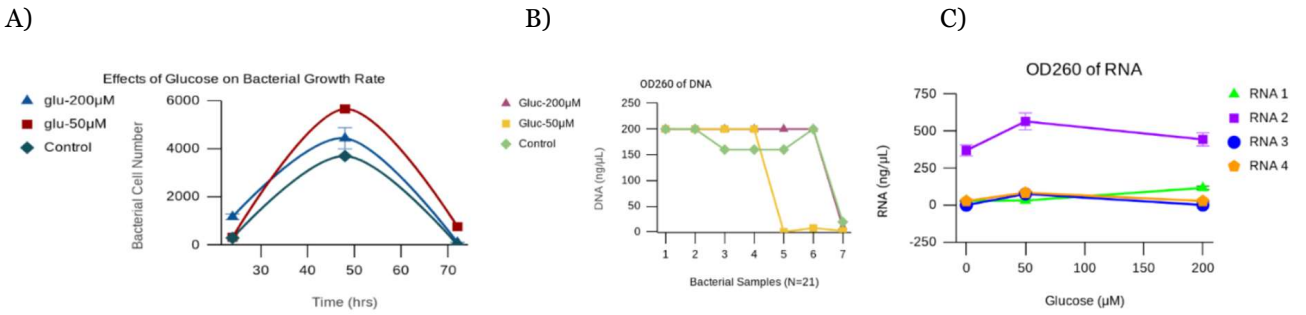

Figure 2. The Effects of Glucose on the Growth Rate and OD260 Results of *E. coli*. A) *E. coli* samples with 50 μM of glucose maintained a higher growth rate **B)** DNA quantification based on OD260 for *E. coli* grown in glucose-enhanced media (200 μM, 50 μM, and 0 μM). **C)** The OD260 results for RNA showed 50 μM of glucose yielded higher levels of RNA at 566 ng/μL than 200 μM of glucose producing 117 ng/μL of RNA with the control limited to 76 ng/μL of an RNA concentration.

glucose in a dosing manner. Then, RNA and *accA* levels were measured. The addition of 50 μM of glucose to the *E. coli* cell samples produced the highest growth rate of *E. coli* (Figure 2a). Bacterial cultures that lacked glucose yielded the lowest *E. coli* cell growth rate (Figure 2a). Figure 2b shows the OD260 DNA results for each bacterial sample treated with 200 μM and 50 μM glucose and appended with control groups. The OD260 DNA analysis of the 200 μM *E. coli* sample showed a sustained and higher rate of nucleic acid production. However, 50 μM glucose produced the highest yield of RNA at 566 ng/μL, while 200 μM glucose yielded 117 ng/μL of RNA, and the control generated 76 ng/μL of RNA (Figure 2c). RNA was then isolated from the sample groups treated with glucose to perform qPCR quantification of *accA* (qPCR-*accA*) and compared to RNA levels in each sample. The glucose amplified RNA and *accA* levels, in which upregulation of *accA* indicates increased FAS activity.

E. coli samples treated with the highest glucose supplementation produced higher levels of RNA and *accA*. The obtained total RNA concentrations were 1392, 797, 608, and 199 ng/μL for H-glucose (15 mM), M-glucose (7.5 mM), L-glucose (5 mM), and the control, respectively (N=25, M=335.4, SD=329.2) (Figure 3a). Similarly, the concentration of *accA* transcripts, as determined by qPCR analysis, was 4210, 375, 1500, and 196 ng/μL for H-glucose, M-glucose, L-glucose, and the control, respectively (Figure 3a). Standard curves were used to perform absolute qPCR quantification of *accA* gene copies with 11-186, 5-18, and 0-79 gene copies observed for H-glucose, M-glucose, and L-glucose/control samples, respectively (n=4, M=48, SD=38). Furthermore, the glucose enhanced *E. coli* samples were compared against samples expressing asRNA *accA* inhibition ((+)-asRNA-*accA*).

In contrast, lowering glucose levels and inhibiting *accA* gene expression can reduce bacterial metabolic activity, such as FASII, in *E. coli*. Bacterial samples that were transformed with pHN1257 vectors for producing *accA* asRNA showed a reduction in RNA with less *accA* gene expression (Figure 3b and Figure 3c). The suppression of *accA* was confirmed by real-time qPCR with a qPCR concentration of 63 ng/μL measured (n=4) as compared to 421.69 ng/μL for *E. coli* samples without asRNA inhibition of *accA* ((-)asRNA-*accA*) (Figure 3d). The obtained total RNA concentrations were 739.44 ng/μL for the control ((-) asRNA-*accA*) and 279.28 ng/μL of RNA for bacteria transformed with pHN1257-(+)asRNA-*accA* plasmids, while the corresponding micro-RNA or miRNA concentrations were 334.98 ng/μL and 240.90 ng/μL, respectively (Figure 3d). There was a 147 percent difference in *accA* qPCR products between (+)asRNA-*accA* bacterial cells and the untransformed control, (95% CI [63, 421.69]). A reduction in glucose and asRNA *accA* gene silencing produced less RNA and yielded less *accA*, which signaled reduced FAS activity in the *E. coli* cell samples.

luxS and *accA*

To determine the effect of *accA* inhibition on *luxS,* the number of *luxS* gene copies was measured by real-time qPCR after inhibiting *accA* while altering glucose (25, 5, and 0 μM). The *luxS* levels were measured in gene copies produced by the absolute quantification following qPCR analysis. A one-way ANOVA statistical test (Table 1 in Supplemental Section) was performed to examine and confirm the current study's hypothesis stating that less glucose and the inhibition of *accA* reduces *luxS* gene expression. Because the independent variable of this method and approach used more than two conditions, a Bonferroni and Holm multiple comparison was implemented to determine which *E. coli* sample treatment groups, when compared to the control groups, were statistically significant with a $P<0.05$ (Table 2 in Supplemental Section).

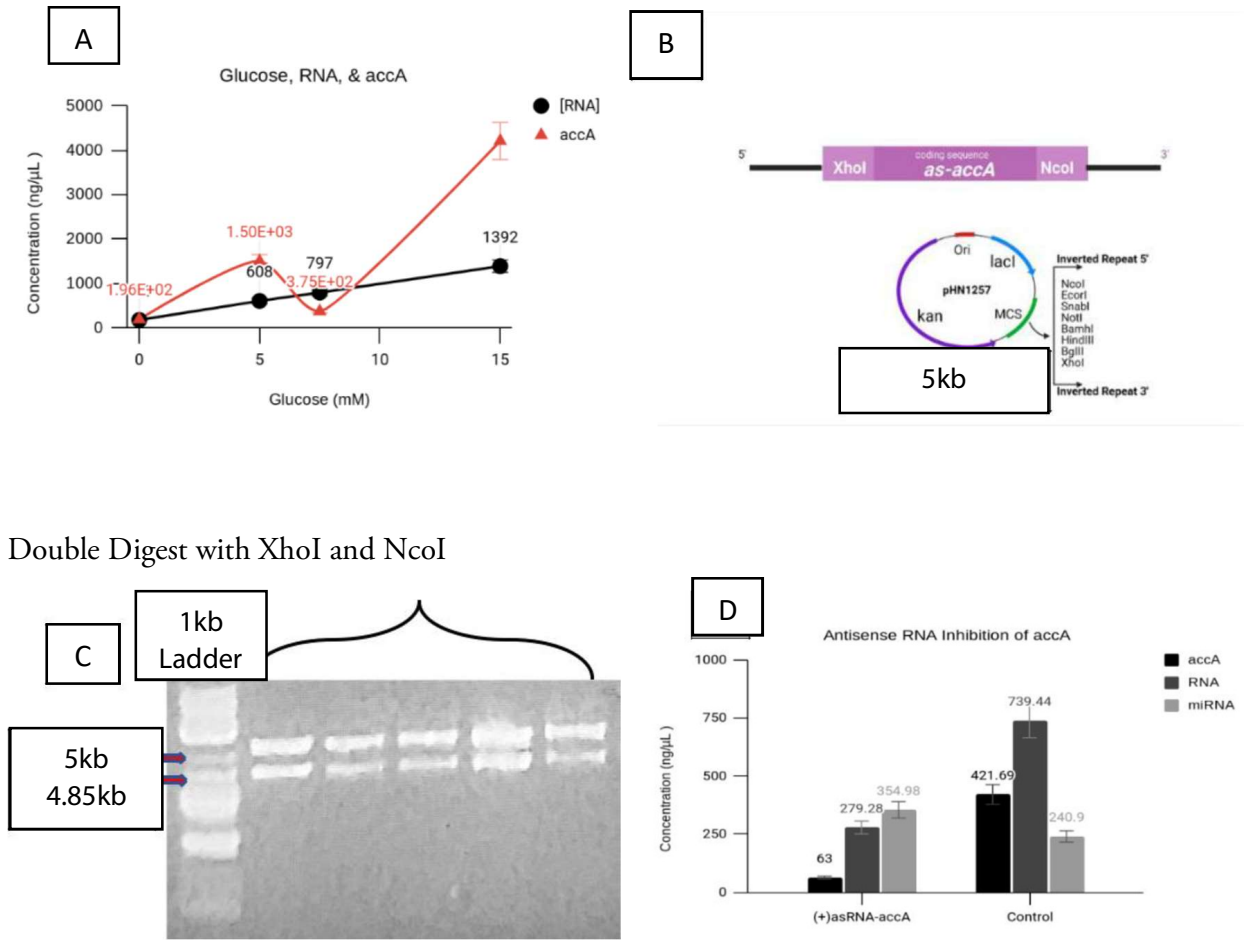

Figure 3: Influence of glucose concentration on RNA transcription and *accA*. Bacteria were cultured with added glucose at a range of concentrations (15 mM, 7.5 mM, 5 mM, or 0 mM). **A)** Direct proportional relationship of *E. coli* total RNA concentration and glucose. The 15mM produced the highest yield of *accA*. **B)** Image shows the asRNA of *accA* and its insertion into the pHN1257-PT-IPTG plasmid of 5,000 base pairs to create inverted antisense repeats for inhibiting *accA* gene expression in *E. coli*. **C)** Image shows agarose gel electrophoresis results of the newly formed recombinant plasmid DNA vector consisting of the asRNA inverted repeats of *accA* after a double restriction digestion, using XhoI and NcoI restriction enzymes. The double digestion of the pHN1257-asRNA-accA plasmid produced two bands at 5 and 4.85 kb, including a 1kb DNA ladder, on a 1% TAE agarose gel. D) pHN1257-asRNA-accA transformants exhibited lesser levels of accA after qPCR analysis with 63 ng/µL. The control yielded higher levels of accA, RNA, and miRNA as compared to the pHN1257-asRNA-accA transformants.

The conditions were significantly different, excluding (+)-asRNA-*accA E. coli* samples treated with 5 µM and 25 µM of glucose, producing p-values>0.05 (Table 2 in Supplemental Section). Because the *luxS* qPCR gene copies, for each sample group, were excessively large values, the raw data were transformed into logarithms (log10). The control samples with (-) glucose-(-) asRNA-*accA* (5.9 ± 0.9), and the 5 µM glucose-(+)asRNA-*accA* (4.7 ± 1.2) exhibited the highest gene copy number for *luxS*. The (-) glucose-(+) asRNA-*accA* sample produced a gene copy number of 199 (2.6 ± 0.5) versus 1 x 10^6 *luxS* copies for the control, (-) glucose- (-) asRNA (5.9 ± 0.9) (Figure 4a-4b).

The difference between the control and the (+)asRNA-*accA* samples for the *luxS* qPCR products was significant (P=0.0291855) (Figure 4c). Figure 4c shows the control group compared to the 5µM-glucose-(+)asRNA-*accA* production of *luxS* was insignificant (P=0.6948811). The control samples compared to the 25µM-glucose-(+) asRNA-*accA E. coli* samples were insignificant (P=0.2662906) (Figure 4c). The asRNA inhibition of *accA* lowered *luxS levels* in the absence of supplemental glucose and the asRNA inhibition of *accA* significantly reduced *luxS*, where a one-way ANOVA computed a p-value<0.05 (F-value=4.1493, P=0.0477) (Table 1 in Supplemental Section). The greatest difference in gene copy values was

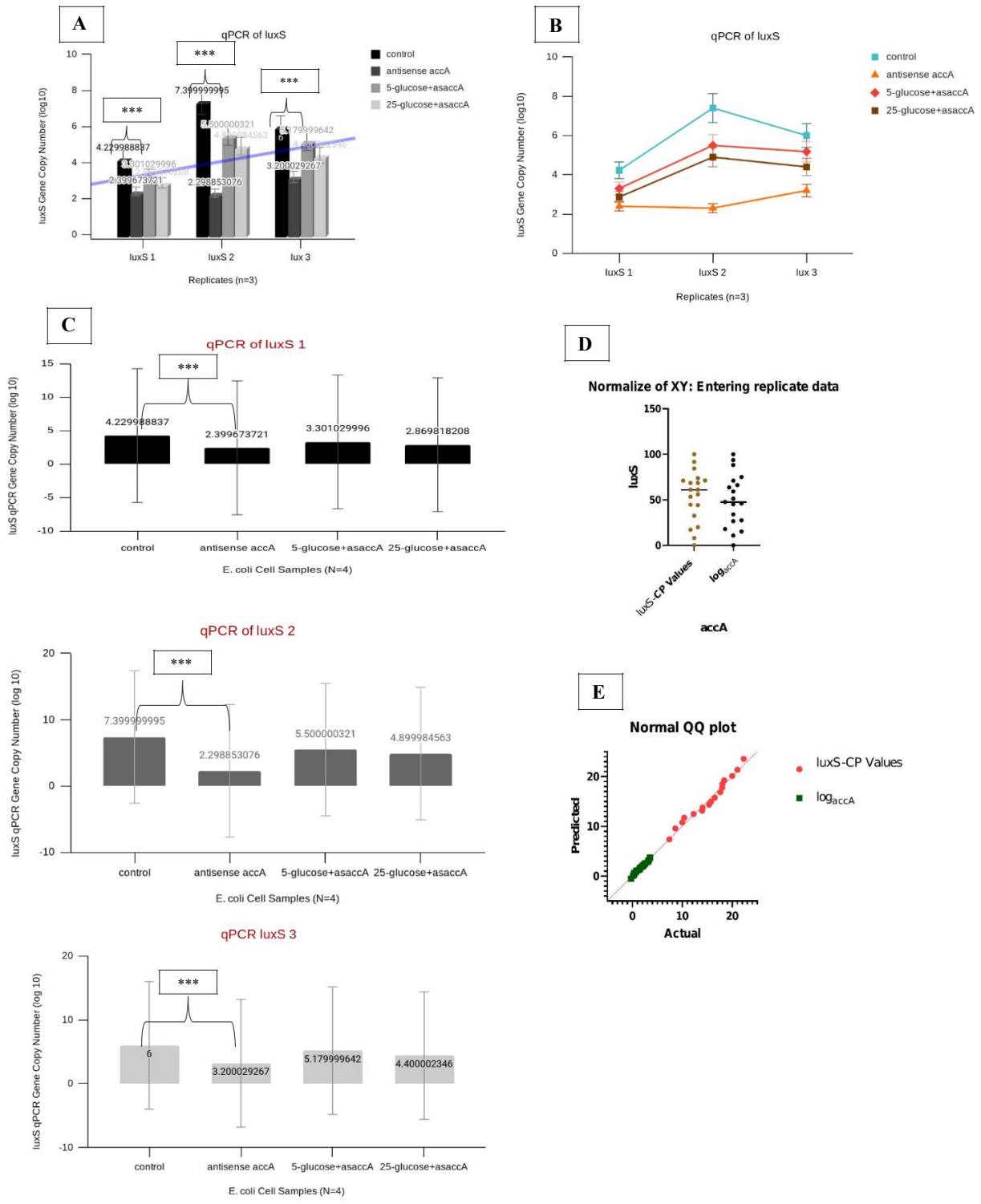

Figure 4: Effect of *accA* asRNA inhibition (log*accA*) on *luxS gene* expression (CP-Values). Transcription of *luxS* exhibits a proportional relation with *accA* levels. **A)** The greatest difference of expression was observed between the control (-) glucose-(-)asRNA and the (+)-asRNA-*accA* sample groups. Inhibition of *accA* by asRNA resulted in tandem reduction of *luxS* expression. **B)** The control samples with (-) glucose-(-) asRNA-*accA* (5.9± 0.9), and the 5µM glucose-(+)asRNA-*accA* (4.7±1.2) exhibited the highest expression of *luxS*. **C)** The greatest difference of expression was observed between the control (-) glucose-(-) asRNA and the (+)-asRNA-*accA* sample groups with $P<0.05$ values **D)** Cp values for *luxS* were parallel to log*accA* data in most replicates. **E)** The QQ plot shows normally distributed means between *luxS* Cp and log*accA* values. (***=p-values<0.05)

observed between the control (-) glucose-(-) asRNA-*accA* and the (+)-asRNA-*accA* sample groups. The *luxS* also exhibited a strong correlation and interaction with *accA*, as shown in a normalization and QQ plot (Figure 4d-4e). Gene inhibition of *accA* lowered *luxS* levels, and the effects of reduced *accA* gene expression on antibiotic resistance were determined.

Antibiotic Resistance Tests

The level of antibiotic resistance was examined using the Kirby-Bauer disk diffusion method for *E. coli* cultures expressing asRNA inhibition of *accA*. An unpaired t-test confirmed the second hypothesis stating that *E. coli* (+)-asRNA-*accA* samples exhibit less resistance to antibiotics because of *accA* inhibition disrupting FAS. Antibiotic resistance was quantified in millimeters (mm) after measuring the zone of inhibition (ZOI) for each antibiotic disk of tetracycline (10 µg/mL), carbenicillin (100 µg/mL), and chloramphenicol (25 µg/mL). All treatments were significantly different. *E. coli* samples exhibiting *accA* suppression (M=21, SD=4, SEM=0.7, N=32) were predominantly susceptible to all three antibiotics (Figure 5A-5B), with an 20mm average zone of inhibition.

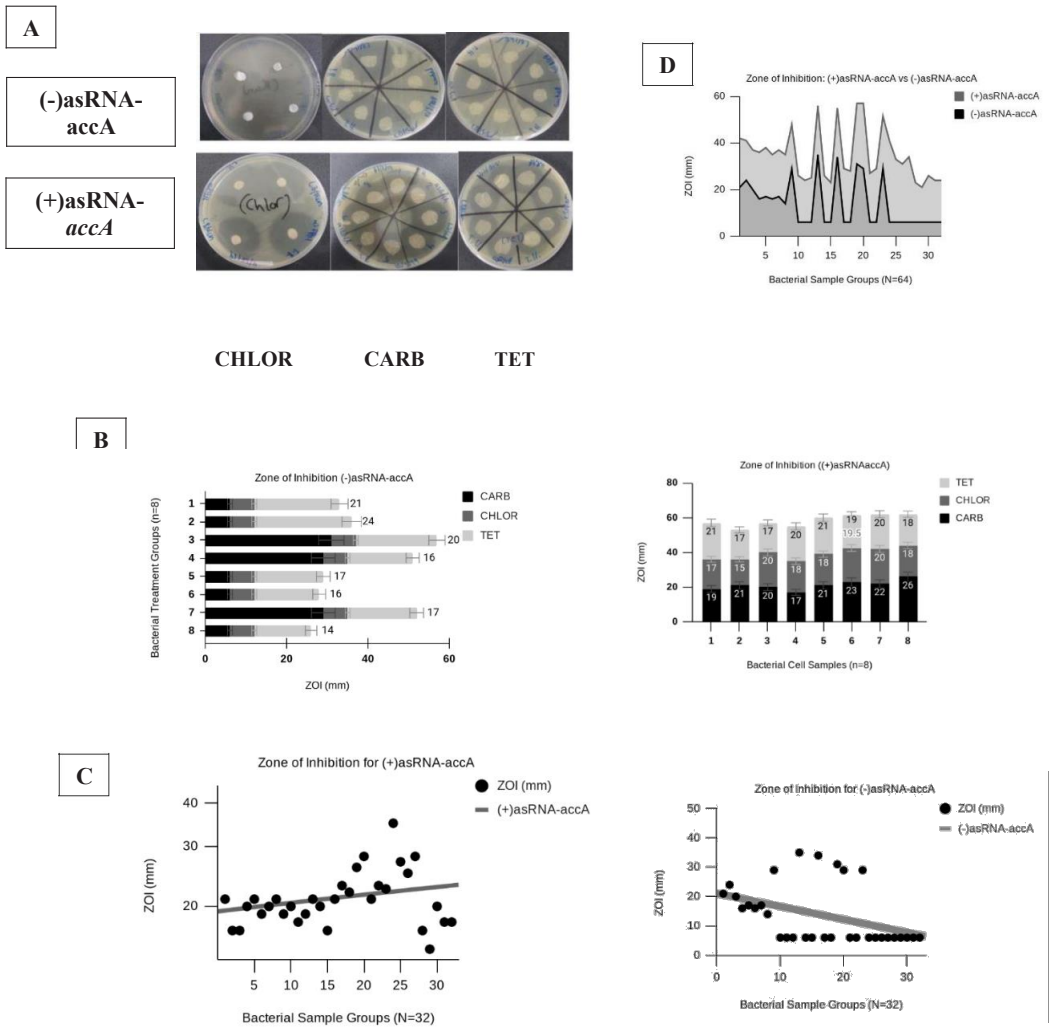

Figure 5: Antibiotic susceptibility testing. A) *E. coli* sample cultures of pHN1257-(+)asRNA-*accA* transformants produced larger zones of inhibition than the control samples following Kirby-Bauer Disk Diffusion antibiotic tests. **B)** Bacteria transformed with pHN1257-(+)asRNA-*accA* showed greater susceptibility to antibiotic disks containing tetracycline (TET), chloramphenicol (CHLOR), and carbenicillin (CARB). **C)** Twenty-seven of the total 64 samples were susceptible; 13 demonstrated intermediate susceptibility; and 18 were resistant. The ratio of zone sizes for (+)asRNA-*accA* to (-)asRNA-*accA* was 3:2. **D**) Zone of inhibition (ZOI) sizes differed by 60% (95% CI, [6,32]) between asRNA-*accA* transformants and controls where transformants yielded larger zones of inhibition.

In contrast, the control samples ((-)asRNA-*accA*) were more resistant to the antibiotics, with an average ZOI of 6 mm (Figure 5A-5B). Ultimately, 59% of (+)asRNA-*accA* samples were sensitive to tetracycline, chloramphenicol, or carbenicillin, showing larger zones of inhibition (Figure 5C). Another 28% of the (+)asRNA-*accA* transformants displayed intermediate sensitivity, while 3% were resistant to antibiotics (13.75±10, SEM=1.8). Control samples exhibited a higher prevalence of resistance, with 25%, 12.5%, and 53% of samples, respectively demonstrating susceptibility, intermediate resistance, and resistance (Figure 5C). Overall, the (+) asRNA-*accA* treatment groups differed from the control group by 82% (95% CI, [6,32]), and the control group varied from the treatment group by 77% (P=0.000554, t-score=3.6, df=31, 95% CI, [6,32]). Overall, Figure 5D shows that (+)-asRNA-*accA*-transformants yielded larger zones of inhibition than the untransformed sample groups.

Discussion

The effect of glucose on RNA levels and *accA*

The aim of the current study was to link bacterial cell metabolism, such as FAS, with bacterial virulence and antibiotic efficacy. MDR-GNBs are more resistant to antibiotics because of their double membrane cell envelope structure. FAS can affect the cell envelope's plasma membrane FA composition, where most bacteria synthesize fatty acids as precursors for forming the cell envelope [32]. For this reason, the current study purposed to confirm the *accA* gene, which codes for the AccA subunit of the CT (AccA-AccD subunits) of the ACCase enzyme, as a potential target for inhibiting FAS. FAS is also intensely regulated in bacterial cells. FAs are produced during FASII in *E. coli*, where the biotin-dependent ACCase enzyme performs a crucial function for catalyzing fatty acid metabolic activity by completing two enzymatic reactions in two half-reaction steps. The first step, catalyzed by biotin carboxylase (BC), is the carboxylation of the N1' atom of a biotin vitamin cofactor, which depends on ATP and carbon dioxide derived from bicarbonate [12]. In this process, biotin covalently bonds to a lysine side chain residue located in the biotin carboxyl carrier protein of the BCCP subunit. Biotin also interacts with the "thumb" of BCCP, a loop of eight amino acids that extends from the C-terminus domain [6] fortifies the BCCP-biotin interaction.

In the second step, a carboxyl transferase (CT) transfers carbon dioxide from the bonded carboxyl-biotin to a carboxyl group. Under increased glucose supplementation, excess carboxyl groups and ATP are available, promoting elevated activity of the BCCP thumb, thus promoting the first carboxylation step in fatty acid synthesis. Glucose is also the source of the carboxyl groups transferred by BCCP to CT. If a carboxyl is not present, biotin cannot attach to the CT subunit [33]. The control sample had a lower value of RNA and *accA* gene expression, which indicated less FAS activity, because without the excess glucose providing the subsequent carboxyl groups, a biotin cannot bind to a CT for transferring carboxyls to acetyl-coA needed for catalyzing FAS. As a result, the *E. coli* samples with the highest concentration of glucose produced increased RNA and *accA*. When *accA* expression is amplified, the activity of the CT enzyme may have surged, specifically transferring more carboxyls to acetyl-CoA molecules for conversion into malonyl-CoA to catalyze FAS.

The phospholipid (PL) bilayer is constructed through the FAS elongation of fatty acids [5] and the translation of *accA* into subunits AccA with AccD of the CT enzyme is needed for FASII catalysis. Blocking phospholipid synthesis leads to a decrease in FAS activity and reduces aggregation of acylated ACP derivatives [34]. Degrading the PL bilayers of the MDR-GNB cell envelope by inhibiting FASII is possible by silencing *accA* gene expression. To confirm the reduction of *accA*, cells were transformed with pHN1257-IPTG-PT-asRNA vectors carrying the inverse insert for asRNA inhibition of *accA*, after which total RNA was extracted and the gene expression of *accA* was quantified by qPCR. The level of *accA* gene expression was substantially reduced to 63 ng/μL, and the reduction of *accA* also lowered the RNA levels of *E. coli* samples, indicating less bacterial growth.

Lessening ACCase activity through *accA* gene inhibition can shorten the length of the acyl chain, which can increase or decrease the elongation. The lipid acyl chains produced during FASII construct more fluid and permeable bacterial cells. Bacterial cells located in biofilms versus planktonic bacterial cells possess higher concentrations of fatty acids [14]. Higher access to fatty acids increases tolerance to various temperatures, more stacking of bacterial cells, and more stable lipid bilayers [14]. The increased presence of long-chain fatty acids leads to an increased orientation of fatty acids in the lipid bilayer, amplifies the links between acyl chains, and stabilizes the lipid bilayer [14]. Thus, inhibiting *accA* encoding the AccA subunit of the CT enzyme can disrupt the elongation of acyl-ACP chains by stagnating FASII. Reduced FAS can degrade the PL that damages the double-membrane cell envelope required for viable and antibiotic-resistant GNB cells.

Real-time qPCR analysis of *luxS* after asRNA *accA* inhibition

Likewise, there is a need to improve our interpretation of the link between AI-2 QS signaling and antibiotic susceptibility, which may also attract increased research interest [29]. Bacterial metabolism is related to virulence;

therefore, inhibiting fatty acid metabolism and targeting other metabolic pathways of MDR-GNB may decrease its pathogenicity and lower antibiotic resistance. Therefore, the present study aimed to demonstrate an interdependent relationship between *accA* and *luxS* to link bacterial fatty acid metabolism with virulence caused by the LuxS/AI-2 QS system in *E. coli*. LuxS is essential for cell growth, quorum sensing, and biofilm formation. The LuxS/AI-2 QS system regulates virulence factors, bacterial bioluminescence, sporulation, toxin production, biofilm formation, and antibiotic resistance [29]. Overall, reducing the activity of the LuxS/AI- 2 system, through suppression of *luxS* via *accA* gene inhibition, can dismantle the biofilm structure and reduce bacterial virulence.

In an intercellular process called quorum sense (QS) signaling, *E. coli* cells release AI-2 signaling molecules to detect cell density and regulate gene expression. In *E. coli*, the transporter and transmembrane complex LsrACDB, an ATP-binding cassette importer, controls AI-2 uptake. LsrACDB contains transmembrane permease proteins, nucleotides for binding proteins, and a periplasmic solute to bind proteins. The repressor of LsrACDB and LsR is a kinase that is part of the QS system of AI-2. Lsrk is a kinase located in the cytoplasm, phosphorylates AI-2, and then Lsrk attaches to the *lsr* repressor. Activated AI-2 suppresses the *lsr* repressor, termed LsrR, leading to increased release of AI-2 via autoinducer-activated expression of the LuxS protein. As the bacterial population increases, AI-2 fills the extracellular space [35-45] for the detection of quorum sensing signals where the bacterial cells can respond to those signals and then alter their gene expression and control the population density [46-51]. Thus, quorum-sense activity monitors and regulates gene expression like a positive feedback loop mechanism that is triggered by the peripheral and internal accumulation of AI-2. The synthesis of AI-2 is ultimately dependent on the expression and translation of *luxS* (Figure 6).

It was hypothesized that *luxS* gene expression declines after suppressing FAS through inhibiting *accA* with asRNAs. This hypothesis was tested and supported by the results showing that asRNA inhibition of *accA* lowered *luxS* levels in the absence of supplemental glucose. The greatest difference in expression was observed between the control (-)glucose-(-)asRNA sample and the (+)asRNA-*accA* samples. Glucose increased the rate of *luxS* transcription, and *luxS* was more amplified in cells with glucose than in cells lacking glucose. Meanwhile, the heightened genetic activity of *luxS* observed upon glucose supplementation both with and without inhibition of *accA* supports the metabolic dependency of the LuxS/AI-2 QS system. For example, the results for the control group versus the 5 μM-glucose-(+)asRNA-*accA* may have been insignificant because, according to Wang et al., adding 0.8% glucose to bacterial cultures and growth medium increases activity at the *luxS* promoter [53]. Wang et al. also found that supplemental glucose increased the levels of AI-2 in culture [53]. However, Jesudhasan et al. demonstrated that when culturing *Salmonella typhimurium* in excess concentrations of glucose, higher levels of autoinducer-2 did not necessarily produce excess *luxS* expression [54]. Hence, increasing the glucose concentration to 25 μM did not significantly amplify *luxS* gene expression.

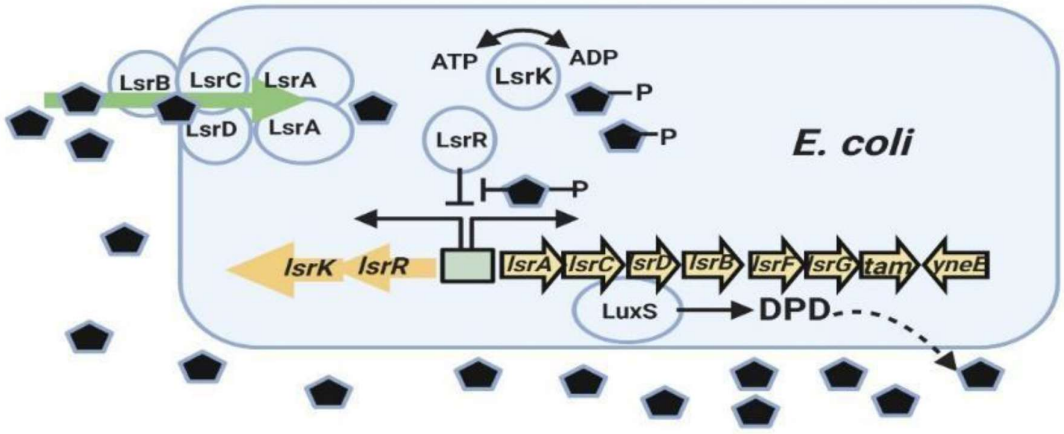

Figure 6: Regulatory mechanisms of the LsrR/phospho-AI-2 system in *E. coli* (produced from reference [52]). The AI-2 (*black pentagons*) uptake repressor LsrR represses the *lsr* operon containing *lsrACDBFG* and the operon of *lsrRK*. AI-2 can re-enter the cell through the expression of LsrACDB. When the LsrK kinase phosphorylates an imported AI-2, the phosphorylated AI-2 binds to LsrR and terminates its repression of *lsr* transporter genes, inducing their expression. These regulatory steps trigger increased AI-2 uptake. (DPD=4,5-dihydroxy-2,3-pentanedione) *** Created with BioRender.com

The integration of bacterial FAS catalysis by the ACCase-AccA-AccD of CT with *luxS* activity was evaluated, where transcription of *luxS* exhibited a proportional relation with *accA* levels. Inhibiting *accA* reduced the activity of the *luxS* promoter in the absence of supplemental glucose, due to reduced fatty acid synthesis. Widmer et al. added glucose and fatty acids to a medium culture of *luxS* mutant *Salmonella Typhimurium* to determine the effects of fatty acids on growth rate and AI-2 [28]. Widmer et al. found that AI-2 enhanced the growth rate of the *luxS* mutant *S. Typhimurium*; however, fatty acids controlled the virulence level of the *luxS* mutant *S. Typhimurium* by regulating AI-2 activity [28]. Jia et al. found that the growth and metabolism of a *luxS* mutant strain of *Lactobacillus plantarum* decreased because FAS was reduced, which then abated cell membrane fluidity [55].

For *E. coli* and other gram-negative bacteria, the fluidity of the membrane is regulated by the ratio of saturated to unsaturated fatty acyl chains in the phospholipids of the membrane [22]. GNB transmembrane proteins are implanted in the hydrophobic interior of the lipid bilayers of the double membrane, and FAS of lipids, including phospholipids, affect the composition of the cell membrane [56-60]. The viscosity (thickness) or fluidity of the lipid bilayer is important for the activity of membrane proteins. Membrane lipid bilayer thickness changes as the membrane fluidity and phases are altered to allocate proteins to different regions and phases of the bacterial cell membrane [61]. The varied configurations of lipids control the physicochemical properties of the cell membrane, such as viscosity, rigidity, phase behavior, and membrane fluidity [62-67]. Unsaturated lipids have a double bond that creates a kink in lipids, which prevents tight lipid packing in the cell membrane and increases fluidity.

It may be inferred that disrupting FASII via *accA* inhibition can form an incomplete GNB double membrane that has less membrane fluidity than needed for the LsrACDB transmembrane protein to operate, thereby impairing the influx of Al-2. This reduced internal AI-2 may have led to the downregulation of *luxS*. Inhibiting *accA* may have produced an incomplete fatty acid elongation cycle where less availability of FAs and acyl groups decreased the fluidity of the cell membrane. Furthermore, incomplete OM and IM, due to *accA* inhibition suppressing FASII catalysis, can permit an elevated influx of antibiotics into the cytoplasm of previously drug-resistant bacteria.

Antibiotic resistance tests

MDR-GNBs are highly resistant to antibiotics because of the double membrane in the cell envelope of GNB, which contains the OM and IM. Because bacterial metabolism and environmental stress play concrete roles in the outcomes of antimicrobial treatments [68], the inhibition of *accA* by asRNA-disrupted FAS and FA elongation may have formed an unstable plasma membrane structure for the *E. coli* cells, allowing a more facile transport of the antibiotics across the OM and IM. The potent metabolic state of a bacterial population can lower bacterial susceptibility to antibiotics [69-75]; therefore, suppressing bacterial metabolism may decrease antibiotic resistance. Consistent with this expectation, the study findings showed that *E. coli* cells expressing (+)asRNA-*accA*, which eliminated the AccA subunit from the ACCase-CT enzyme, were more susceptible to antibiotics. These results support the hypothesis that silencing the gene *accA* lowers the antibiotic resistance of the *E. coli* bacterial cells. Furthermore, less FASII activity may have degraded the IM and OM of the (+)asRNA-*accA E. coli* cells, and the damaged cell envelope of the *E. coli* cells may have allowed a greater influx of antibiotics.

A fully assembled OM is required for a viable gram-negative bacterial cell to remain resistant to antibiotics; therefore, designing therapeutics to inhibit OM assembly can kill bacteria and sensitize them to antibiotics [76]. The OM composition is essential for its ability to function as a barrier. OM is composed of an inner phospholipid bilayer and an outer leaflet of glycolipids termed lipopolysaccharides (LPS). OM also consists of outer membrane proteins (OMPs) such as lipoproteins. The lipid molecules of the OM are formed in the IM and require delivery from the IM, pass through the periplasmic space, and then enter the OM. The LPS is composed of glycolipids that protects the OM against both hydrophilic and hydrophobic antibiotic types. LPS contains lipid A. Lipid A, which consists of four to seven saturated acyl chains, are anchored into the bilayer. Oligosaccharide cores are bound to lipid A. For the LPS to fully function, it must be synthesized and traversed across the periplasm [76]. Lipid A, which is attached to the core oligosaccharide regions of LPS, is formed in the cytoplasmic regions of the IM, and the molecules are transported through the periplasmic space into the OM bilayer leaflet.

Lipoproteins are triacylated proteins. Without the movement of lipoproteins, the OM of gram-negative bacteria cannot be assembled [76]. Inhibiting the assembly and trafficking of lipoproteins can kill GNB cells or permeabilize the GNB protective cell envelope to antibiotics that cannot cross the OM [76]. When acyl groups are fully added to lipoproteins, they can be transported to the OM. Only mature triacylated lipoproteins can be transported to the OM; therefore, a possible method to inhibit lipoprotein trafficking is to block the maturation or acylation of lipoproteins in the IM [76]. Currently, no antibiotics have been designed to target the OM assembly [76].

However, this study showed promising results that inhibiting *accA* of the ACCase-CT enzyme can disrupt

FASII of acyl-ACP groups in *E. coli*. It may be inferred that inhibiting *accA* can block the synthesis of saturated acyl chains by reducing FASII, which is required for the formation of lipid A to be transported across the IM into the OM. A lack of saturated acyl groups from FASII can prevent the transport of lipid A into the OM to form a resistant barrier to antibiotics. Lipoproteins are required for full assembly of OM. Blocking *accA* synthesis and FASII limited the availability of acyl groups, which may have prevented the full maturation of lipoproteins needed for its trafficking into the OM of the *E. coli* sample cells. Inhibiting FASII catalysis by blocking gene expression of *accA*, may lessen access to acyl groups needed for lipid A and lipoprotein formation. A decreased amount of acyl groups may have inhibited the assembly of the OM and permeabilized the *E. coli* cell samples to a greater influx of antibiotics, as confirmed in this study's antibiotic resistance tests. The gene inhibition of *accA* has the potential to develop effective antimicrobial gene therapies for permeabilizing MDR-GNB cells to increase antibiotic uptake.

Conclusion

Multidrug-resistant gram-negative bacteria have created an intense challenge for clinicians treating infections of ill patients in intensive care units [77]; however, in recent years, GNB has become resistant to all common categories of antimicrobials [77]. During the past 30 years, the formulation and discovery of potent antibiotics have dwindled [78]. The higher rate of multiple resistance among GNB is partially attributable to their double-membrane cell envelope that comprises an OM consisting of LPS with endotoxins, a peptidoglycan cell wall, and an inner phospholipid membrane. The outer membrane can also restrict the penetration of antibiotics into the GNBs [79]. Many new and novel antibiotics have been produced in recent years to combat gram-positive bacteria [80]; however, administration of these novel antibiotics has been limited to decrease the occurrence of MDR. Combined with the rise of MDR-GNB, this limitation has forced the administration of older antibiotics such as polymyxins B and E [81]. Antimicrobial peptides (AMPs) have been considered as an alternative novel approach because of their degrading bacterial structure through direct electrostatic interactions with microbial membranes [82]; however, many AMPs have failed to achieve success in clinical studies because they are toxic to mammalian cells.

Nonetheless, the current study presented significant results concerning the effect of *accA* inhibition along with glucose supplementation on the expression of *luxS*, an essential component in bacterial biofilm formation, quorum sensing, and virulence. The hypothesis that silencing *accA* lowers *luxS* gene expression was confirmed by the results. Inhibiting *accA* reduced *luxS* gene *expression*, which was confirmed by real-time qPCR analysis. Importantly, suppressing *accA* can lessen the virulence of pathogenic bacteria by disrupting the LuxS/AI-2 QS system responsible for biofilm formation. The suppression of *luxS* was attributed to *accA* inhibition disrupting FAS, which lowers cell membrane fluidity. Cell membrane fluidity affects the structure and function of bacterial membrane proteins. Less cell membrane fluidity may have denatured the LsrACDB transmembrane protein conformation, limiting AI-2 uptake that decreased Lux-S activity. However, the current study's findings were limited in that the addition of glucose continued to amplify *luxS* gene copy numbers after asRNA inhibition of *accA*. The 5 μM and 25 μM of glucose increased *luxS* levels because glucose stimulates activity of the *luxS* promoter site according to Wang et al. [53], and glucose concentration varies *in vivo*. Therefore, before using inhibitors of *accA* as an antimicrobial gene therapy, further research is necessary for extensively determining the effectiveness of *accA* gene inhibition *in vivo*. The antibiotic resistance tests, implementing the selected antibiotics, exhibited higher rates of susceptibility for (+)-asRNA-*accA* cell cultures because the inhibition of *accA* disrupted fatty acid production, which may have damaged the OM and IM cell envelope structures, increasing the influx of antibiotics.

The second hypothesis was confirmed by the results where antibiotic resistance was minimized in (+)asRNA-*accA E. coli* cell samples. Inhibiting *accA* suppresses acyl-ACP production required for lipid A and lipoprotein formation in the OM. Degradation of the OM may have occurred and caused an elevated influx of antibiotics into the (+)asRNA-*accA E. coli* cell samples. Many bacteria and plants form fatty acids using the conserved FASII enzymes. The bacterial FASII enzymes structurally differ from mammalian FASI enzymes that complete FAS via a single polypeptide with multiple functions [15]. As a result, targeting bacterial FASII enzymes is highly favorable because FASII enzyme inhibitors cannot affect mammalian FASI enzymes. The current study provides support for antimicrobial gene therapies targeting *accA*. Targeting *accA* and other bacterial metabolic genes may provide a potent novel antimicrobial therapy against MDR-GNB because the DNA sequence and structure of the AccA-AccD of the CT enzyme is conserved across many different bacterial species [12], can block FASII catalysis, downregulate the LuxS/AI-2 QS system, and reduce antibiotic resistance.

Hall et al. concluded that the cause of antibiotic resistance or antibiotic sensitivity of biofilms originates from a genetic source [83]; therefore, perhaps combating MDR-GNB requires a gene-based antimicrobial approach, as shown in

the current study. The findings of this study demonstrate that *accA* is a favorable target for antimicrobial gene therapy development. This study's findings include the interaction between fatty acid metabolism and virulence, which may serve as a step to inform our understanding metabolic-dependent pathogenesis in bacteria. Building on this work could ultimately lead to further studies that confirm the significant antimicrobial potency of silencing *accA* genes as an antibiotic gene therapy for MDR-GNB infections. Future studies could silence *accA* genes with small interfering RNAs or clustered regularly interspaced short palindromic repeats, such as CRISPR-Cas9 nucleases. *In vivo* assays of humanized mice could be used to establish *accA* gene silencing as beneficial and to determine the most effective methods for the delivery of *accA* antimicrobial gene inhibitors.

Acknowledgements

Special thanks are given to the staff of TheLab in Los Angeles, CA. Thank you for your team. They were always available to answer questions and provide support.

Author Contribution

The author confirms sole responsibility for the following: study conception and design, data collection, analysis and interpretation of results, and manuscript preparation.

Conflicts of Interest

The author declares there are no conflicts of interest.

Data Access Statement

Data available on request from the authors.

Ethical Statement

This article does not contain any studies involving animals performed by any of the authors. This article does not contain any studies involving human participants performed by any of the authors.

References

1. Eichenberger EM, Thaden JT. Epidemiology and Mechanisms of Resistance of Extensively Drug Resistant Gram-Negative Bacteria. Antibiotics. 2019 Jun;8(2):37.

2. Alexopoulou A, Papadopoulos N, Eliopoulos DG, Alexaki A, Tsiriga A, Toutouza M, Pectasides D. Increasing frequency of gram-positive cocci and gram-negative multidrug-resistant bacteria in spontaneous bacterial peritonitis. Liver International. 2013 Aug;33(7):975-81.

3. Vergidis PI, Falagas ME. Multidrug-resistant Gram-negative bacterial infections: the emerging threat and potential novel treatment options. Curr Opin Investig Drugs. 2008 Feb;9(2):176-83. PMID: 18246520.

4. Silhavy TJ, Kahne D, Walker S. The bacterial cell envelope. Cold Spring Harbor Perspectives in Biology. 2010 May 1;2(5):a000414.

5. Richie DL, Wang L, Chan H, De Pascale G, Six DA, Wei JR, Dean CR. A pathway-directed positive growth restoration assay to facilitate the discovery of lipid A and fatty acid biosynthesis inhibitors in Acinetobacter baumannii. PloS one. 2018 Mar 5;13(3):e0193851.

6. Broussard TC, Kobe MJ, Pakhomova S, Neau DB, Price AE, Champion TS, et al. The three-dimensional structure of the biotin carboxylase-biotin carboxyl carrier protein complex of E. coli acetyl-CoA carboxylase. Structure. 2013 Apr 2;21(4):650-7.

7. Mochalkin I, Miller JR, Evdokimov A, Lightle S, Yan C, Stover CK, et al. Structural evidence for substrate-induced synergism and half-sites reactivity in biotin carboxylase. Protein Science. 2008 Oct;17(10):1706-18.

8. Meades Jr G, Benson BK, Grove A, Waldrop GL. A tale of two functions: enzymatic activity and translational repression by carboxyltransferase. Nucleic acids research. 2010 Mar 1;38(4):1217-27.

9. Kondo S, Nakajima Y, Sugio S, Sueda S, Islam MN, Kondo H. Structure of the biotin carboxylase domain of pyruvate carboxylase from Bacillus thermodenitrificans. Acta Crystallographica Section D: Biological Crystallography. 2007 Aug 1;63(8):885-90.

10. Wunnicke D, Sezgin E, Hänelt I, Ernst R, Doktorova M, Reinhard J, et al. Regulation of lipid saturation without sensing membrane fluidity. Nature Communications. 2020 Feb 6;11.

11. Broussard TC, Price AE, Laborde SM, Waldrop GL. Complex formation and regulation of Escherichia coli acetyl-CoA carboxylase. Biochemistry. 2013 May 14;52(19):3346-57.

12. Tong L. Structure and function of biotin-dependent carboxylases. Cellular and Molecular Life Sciences. 2013 Mar;70(5):863-91.

13. Janiyani K, Bordelon T, Waldrop GL, Cronan Jr JE. Function of Escherichia coli biotin carboxylase requires catalytic activity of both subunits of the homodimer. Journal of Biological Chemistry. 2001 Aug 10;276(32):29864-70.

14. Wang C, Rajput S, Watabe K, Liao DF, Cao D. Acetyl-

CoA carboxylase-alpha as a novel target for cancer therapy. Front Biosci. 2010 Jan 1;2:15-26.

15. Reddy MC, Breda A, Bruning JB, Sherekar M, Valluru S, Thurman C, et al. Structure, activity, and inhibition of the carboxyltransferase β-subunit of acetyl coenzyme A carboxylase (AccD6) from Mycobacterium tuberculosis. Antimicrobial Agents and Chemotherapy. 2014 Oct;58(10):6122.

16. Lu H. Mechanism and inhibition of bacterial enoyl-ACP reductases: Towards novel antibacterial drugs (Doctoral dissertation, The Graduate School, Stony Brook University: Stony Brook, NY.) 2010.

17. Venter H. Reversing resistance to counter antimicrobial resistance in the World Health Organisation's critical priority of most dangerous pathogens. Bioscience Reports. 2019 Apr 30;39(4).

18. Stokes JM, Lopatkin AJ, Lobritz MA, Collins JJ. Bacterial metabolism and antibiotic efficacy. Cell Metabolism. 2019 Aug 6;30(2):251-9.

19. Charles O. Exogenous fatty acid metabolism in bacteria. Biochimie. 2017.

20. Gianotti A, Serrazanetti D, Kamdem SS, Guerzoni ME. Involvement of cell fatty acid composition and lipid metabolism in adhesion mechanism of Listeria monocytogenes. International Journal of Food Microbiology. 2008 Mar 31;123(1-2):9-17.

21. Hurdle JG, O'neill AJ, Chopra I, Lee RE. Targeting bacterial membrane function: an underexploited mechanism for treating persistent infections. Nature Reviews Microbiology. 2011 Jan;9(1):62-75.

22. Baek SH, Li AH, Sassetti CM. Metabolic regulation of mycobacterial growth and antibiotic sensitivity. PLoS Biol. 2011 May 24;9(5):e1001065.

23. Yang JH, Bhargava P, McCloskey D, Mao N, Palsson BO, Collins JJ. Antibiotic-induced changes to the host metabolic environment inhibit drug efficacy and alter immune function. Cell Host & Microbe. 2017 Dec 13;22(6):757-65.

24. Greulich P, Scott M, Evans MR, Allen RJ. Growth-dependent bacterial susceptibility to ribosome-targeting antibiotics. Molecular Systems Biology. 2015 Mar;11(3):796.

25. Lee HH, Collins JJ. Microbial environments confound antibiotic efficacy. Nature Chemical Biology. 2012 Jan;8(1):6-9.

26. Lobritz MA, Belenky P, Porter CB, Gutierrez A, Yang JH, Schwarz EG, Dwyer DJ, Khalil AS, Collins JJ. Antibiotic efficacy is linked to bacterial cellular respiration. Proceedings of the National Academy of Sciences. 2015 Jul 7;112(27):8173-80.

27. Passalacqua KD, Charbonneau ME, O'riordan MX. Bacterial metabolism shapes the host–pathogen interface. Virulence Mechanisms of Bacterial Pathogens. 2016 Jun 22:15-41.

28. Widmer KW, Jesudhasan P, Pillai SD. Fatty acid modulation of autoinducer (AI-2) influenced growth and macrophage invasion by Salmonella Typhimurium. Foodborne Pathogens and Disease. 2012 Mar 1;9(3):211-7.

29. Wang Y, Liu B, Grenier D, Yi L. Regulatory mechanisms of the LuxS/AI-2 system and bacterial resistance. Antimicrobial Agents and Chemotherapy. 2019 Oct 1;63(10):e01186-19.

30. Nakashima N, Tamura T. Conditional gene silencing of multiple genes with antisense RNAs and generation of a mutator strain of Escherichia coli. Nucleic Acids Research. 2009 Aug 1;37(15):e103.

31. Clinical and Laboratory Standards Institute (CLSI). Performance Standards for Antimicrobial Susceptibility Testing. 29th ed. Pennsylvania: Clinical and Laboratory Standard Institute. 2019.

32. Lu X, Vora H, Khosla C. Overproduction of free fatty acids in E. coli: implications for biodiesel production. Metab Eng. 2008 Nov;10(6):333-9

33. Lietzan AD, Maurice MS. A substrate-induced biotin binding pocket in the carboxyltransferase domain of pyruvate carboxylase. Journal of Biological Chemistry. 2013 Jul 5;288(27):19915-25.

34. Marrakchi H, Zhang YM, Rock CO. Mechanistic diversity and regulation of Type II fatty acid synthesis. Biochemical Society Transactions. 2002 Nov;30(6):1050-5.

35. Freestone ST, Bassler BL. Bacterial Quorum Sensing: Its Role in Virulence and Possibilities for Its Control. Cold Spring Harbor Perspectives in Medicine. 2012;2(11): a012427.

36. Li YH, Tian X. Quorum sensing and bacterial social interactions in biofilms. Sensors. 2012 Mar;12(3):2519-38.

37. Jimenez PN, Koch G, Thompson JA, Xavier KB, Cool RH, Quax WJ. The multiple signaling systems regulating virulence in Pseudomonas aeruginosa. Microbiology and Molecular Biology Reviews. 2012 Mar 1;76(1):46-65.

38. Galloway WR, Hodgkinson JT, Bowden SD, Welch M, Spring DR. Quorum sensing in Gram-negative bacteria: small-molecule modulation of AHL and AI-2 quorum sensing pathways. Chemical Reviews. 2011 Jan 12;111(1):28-67.

39. Schuster M, Joseph Sexton D, Diggle SP, Peter Greenberg E. Acyl-homoserine lactone quorum sensing: from evolution to application. Annual Review of Microbiology. 2013 Sep 8;67:43-63.

40. Antunes LC, Ferreira RB, Buckner MM, Finlay BB. Quorum sensing in bacterial virulence. Microbiology. 2010 Aug 1;156(8):2271-82.

41. Novick RP, Geisinger E. Quorum sensing in staphylococci. Annual Review of Genetics. 2008 Dec 1;42:541-64.

42. Kalia VC. Quorum sensing inhibitors: an overview. Biotechnology advances. 2013 Mar 1;31(2):224-45.

43. LaSarre B, Federle MJ. Exploiting quorum sensing to confuse bacterial pathogens. Microbiology and Molecular Biology Reviews. 2013 Mar 1;77(1):73-111.

44. O'Loughlin CT, Miller LC, Siryaporn A, Drescher K, Semmelhack MF, Bassler BL. A quorum-sensing inhibitor blocks Pseudomonas aeruginosa virulence and biofilm formation. Proceedings of the National Academy of Sciences. 2013 Oct 29;110(44):17981-6.

45. Papenfort K, Bassler BL. Quorum sensing signal–response systems in Gram-negative bacteria. Nature Reviews Microbiology. 2016 Sep;14(9):576.

46. Waters CM, Bassler BL. Quorum sensing: cell-to-cell communication in bacteria. Annu Rev Cell Dev Biol. 2005;21:319-346.

47. Hughes DT, Sperandio V. Inter-kingdom signalling: communication between bacteria and their hosts. Nature Reviews Microbiology. 2008 Feb;6(2):111-20.

48. Joint I, Tait K, Callow ME, Callow JA, Milton D, Williams P, et al. Cell-to-cell communication across the prokaryote-eukaryote boundary. Science. 2002 Nov 8;298(5596):1207-.

49. Fuqua C, Parsek MR, Greenberg EP. Regulation of gene expression by cell-to-cell communication: acyl-homoserine lactone quorum sensing. Annual Review of Genetics. 2001 Dec;35(1):439-68.

50. Visick KL, Fuqua C. Decoding microbial chatter: cell-cell communication in bacteria. Journal of Bacteriology. 2005 Aug 15;187(16):5507-19.

51. Von Bodman SB, Willey JM, Diggle SP. Cell-cell communication in bacteria: united we stand. Journal of Bacteriology. 2008 Jul 1;190(13):4377-91.

52. Li J, Attila C, Wang L, Wood TK, Valdes JJ, Bentley WE. Quorum sensing in Escherichia coli is signaled by AI-2/LsrR: effects on small RNA and biofilm architecture. Journal of Bacteriology. 2007 Aug;189(16):6011.

53. Wang L, Hashimoto Y, Tsao CY, Valdes JJ, Bentley WE. Cyclic AMP (cAMP) and cAMP receptor protein influence both synthesis and uptake of extracellular autoinducer 2 in Escherichia coli. Journal of Bacteriology. 2005;187(6):2066-2076.

54. Jesudhasan PR, Cepeda ML, Widmer K, Dowd SE, Soni KA, Hume ME, et al. Transcriptome analysis of genes controlled by luxS/autoinducer-2 in Salmonella Enterica serovar Typhimurium. Foodborne Pathogens and Disease.2010;7(4):399-410.

55. Jia FF, Pang XH, Zhu DQ, Zhu ZT, Sun SR, Meng XC. Role of the luxS gene in bacteriocin biosynthesis by Lactobacillus plantarum KLDS1. 0391: A proteomic analysis. Scientific Reports. 2017 Oct 24;7(1):1-4.

56. Pisithkul T, Schroeder JW, Trujillo EA, Yeesin P, Stevenson DM, Chaiamarit T, et al. Metabolic remodeling during biofilm development of Bacillus subtilis. MBio. 2019;10(3):e00623-19.

57. Federle MJ. Autoinducer-2-based chemical communication in bacteria: complexities of interspecies signaling. Bacterial Sensing and Signaling. 2009;16:18-32.

58. Federle MJ, Bassler BL. Interspecies communication in bacteria. The Journal of Clinical Investigation. 2003 Nov 1;112(9):1291-9.

59. Hirakawa H, Tomita H. Interference of bacterial cell-to-cell communication: a new concept of antimicrobial chemotherapy breaks antibiotic resistance. Frontiers in Microbiology. 2013 May 13;4:114.

60. Demuth DR, Lamont R, editors. Bacterial cell-to-cell communication: role in virulence and pathogenesis. Cambridge University Press; 2006 Feb 23.

61. Gorhbandt M, Lipski A, Baig Z, Walter S, Kurre R, Strahl H, et al. Low membrane fluidity triggers lipid phase separation and protein segregation in vivo. BioRxiv. 2019 Jan 1:852160.

62. Ballweg S, Ernst R. Control of membrane fluidity: the OLE pathway in focus. Biological Chemistry. 2017 Feb 1;398(2):215-28.

63. Thibault G, Shui G, Kim W, McAlister GC, Ismail N, Gygi SP, et al. The membrane stress response buffers lethal effects of lipid disequilibrium by reprogramming the protein homeostasis network. Molecular Cell. 2012 Oct 12;48(1):16-27.

64. Stordeur C, Puth K, Sáenz JP, Ernst R. Crosstalk of lipid and protein homeostasis to maintain membrane function. Biological Chemistry. 2014 Mar 1;395(3):313-26.

65. Surma MA, Klose C, Peng D, Shales M, Mrejen C, Stefanko A, et al. A lipid E-MAP identifies Ubx2 as a critical regulator of lipid saturation and lipid bilayer stress. Molecular Cell. 2013 Aug 22;51(4):519-30.

66. Ernst R, Ballweg S, Levental I. Cellular mechanisms of physicochemical membrane homeostasis. Current Opinion in Cell Biology. 2018 Aug 1;53:44-51.

67. Covino R, Ballweg S, Stordeur C, Michaelis JB, Puth K, Wernig F, et al. A eukaryotic sensor for membrane lipid saturation. Molecular Cell. 2016 Jul 7;63(1):49-59.

68. Kénanian G, Morvan C, Weckel A, Pathania A, Anba-Mondoloni J, Halpern D, et al. Permissive fatty acid incorporation promotes staphylococcal adaptation to FASII antibiotics in host environments. Cell Reports. 2019 Dec 17;29(12):3974-82.

69. Jayaraman A, Wood TK. Bacterial quorum sensing: signals, circuits, and implications for biofilms and disease. Annu Rev Biomed Eng. 2008 Aug 15;10:145-67.

70. Vadia S, Jessica LT, Lucena R, Yang Z, Kellogg DR, Wang JD, et al. Fatty acid availability sets cell envelope capacity and dictates microbial cell size. Current Biology. 2017 Jun 19;27(12):1757-67.

71. Ronald PC. Small protein-mediated quorum sensing in a gram-negative bacterium: novel targets for control of infectious disease. Discovery Medicine. 2011 Dec 1;12(67):461-70.

72. Wood TK, Hong SH, Ma Q. Engineering biofilm formation and dispersal. Trends in Biotechnology. 2011 Feb 1;29(2):87-94.

73. Bhardwaj AK, Vinothkumar K, Rajpara N. Bacterial quorum sensing inhibitors: attractive alternatives for control of infectious pathogens showing multiple drug resistance. Recent Patents on Anti-infective Drug Discovery. 2013 Apr 1;8(1):68-83.

74. Lazãr V, Chifiriuc MC. Architecture and physiology of microbial biofilms. Roum Arch Microbiol Immunol. 2010 Apr;69(2):95-107.

75. Hurdle JG, O'neill AJ, Chopra I, Lee RE. Targeting bacterial membrane function: an underexploited mechanism for treating persistent infections. Nature Reviews Microbiology. 2011 Jan;9(1):62-75.

76. Lehman KM, Grabowicz M. Countering gram-negative antibiotic resistance: recent progress in disrupting the outer membrane with novel therapeutics. Antibiotics. 2019 Dec;8(4):163.

77. Bassetti M, Peghin M, Vena A, Giacobbe DR. Treatment of infections due to MDR Gram-negative bacteria. Frontiers in medicine. 2019 Apr 16;6:74.

78. Polyak SW, Abell AD, Wilce MC, Zhang L, Booker GW. Structure, function, and selective inhibition of bacterial acetyl-CoA carboxylase. Applied microbiology and biotechnology. 2012 Feb 1;93(3):983-92.

79. Exner M, Bhattacharya S, Christiansen B, Gebel J, Goroncy-Bermes P, Hartemann P, et al. Antibiotic resistance: What is so special about multidrug-resistant Gram-negative bacteria. GMS Hygiene and Infection Control. 2017;12

80. Giamarellou H. Multidrug-resistant Gram-negative bacteria: how to treat and for how long. International Journal of Antimicrobial Agents. 2010 Dec 1;36:S50-4.

81. Falagas ME, Kasiakou SK, Saravolatz LD. Colistin: the revival of polymyxins for the management of multidrug-resistant gram-negative bacterial infections. Clinical Infectious Diseases. 2005 May 1;40(9):1333-41.

82. Lam SJ, O'Brien-Simpson NM, Pantarat N, Sulistio A, Wong EH, Chen YY, et al. Combating multidrug-resistant Gramnegative bacteria with structurally nanoengineered antimicrobial peptide polymers. Nature Microbiology. 2016 Sep 12;1(11):1-1.

83. Hall CW, Mah TF. Molecular mechanisms of biofilm-based antibiotic resistance and tolerance in pathogenic bacteria. FEMS Microbiology Reviews. 2017 Mar 25;41(3):276-301.